



Published in final edited form as:

Nature. 2010 February 11; 463(7282): 775–780. doi:10.1038/nature08748.

Rfx6 Directs Islet Formation and Insulin Production in Mice and Humans

Stuart B. Smith¹, Hui-Qi Qu^{2,*}, Nadine Taleb^{2,*}, Nina Kishimoto^{1,*}, David W. Scheel^{1,*}, Yang Lu², Ann-Marie Patch³, Rosemary Grabs², Juehu Wang¹, Francis C. Lynn^{1,4}, Takeshi Miyatsuka¹, John Mitchell², Rina Seerke¹, Julie Désir⁵, Serge Vanden Eijnden⁵, Marc Abramowicz⁵, Nadine Kacet⁶, Jacques Weill⁶, Marie-Ève Renard⁶, Mattia Gentile⁷, Inger Hansen⁸, Ken Dewar⁹, Andrew T. Hattersley³, Rennian Wang¹⁰, Maria E. Wilson¹¹, Jeffrey D. Johnson¹¹, Constantin Polychronakos^{2,13}, and Michael S. German^{1,12,13}

¹Diabetes Center, University of California San Francisco, San Francisco, CA 94143, U.S.A.

²Departments of Paediatrics and Human Genetics, McGill University, Montreal, Québec, Canada

³Institute of Biomedical and Clinical Science, Peninsula Medical School, Exeter, UK

⁵Laboratory of Medical Genetics, Hôpital Erasme-ULB, Brussels, Belgium

⁶Department of Neonatology, Hôpital Calmette, Lille, France

⁷Medical Genetic Unit, Di Venere General Hospital, Bari, Italy

⁸Department of Pediatrics, Emory University School of Medicine, Atlanta, GA, USA

⁹Department of Human Genetics, McGill University, and Research Institute of the McGill University Health Centre, Montreal, Quebec, Canada

¹⁰Departments of Physiology, Pharmacology & Medicine, Child Health Research Institute, the University of Western Ontario, London, Ontario, Canada

¹¹Metabolex Inc., Hayward, CA 94545, U.S.A.

Users may view, print, copy, download and text and data- mine the content in such documents, for the purposes of academic research, subject always to the full Conditions of use: http://www.nature.com/authors/editorial_policies/license.html#terms

¹³Corresponding authors: Constantin Polychronakos, M.D. McGill University Health Center (Children's Hospital), 2300 Tupper, Montréal, Qc, Canada, H3H 1P3 Tel: (514) 412 4315; Fax: (514) 412 4264 Constantin.Polychronakos@McGill.ca Michael S. German, M.D. UCSF Diabetes Center, University of California San Francisco, 513 Parnassus Avenue, San Francisco, CA 94143-0534 Tel: (415) 476-9262; Fax: (415) 731-3612 mgerman@diabetes.ucsf.edu.

*These authors contributed equally to the work.

•These authors contributed equally to the work.

⁴Current address: Departments of Surgery and Cellular and Physiological Sciences, Faculty of Medicine, University of British Columbia, British Columbia, Canada

Author contributions S.B.S., H.Q.Q., N.T., N.Kishimoto, D.W.S., F.C.L., K.D., R.W., C.P., and M.S.G. wrote the paper. K.D., C.P. and M.S.G. oversaw the studies.

S.B.S., D.W.S., Y.L., J.W., T.M., R.W., M.E.W. and J.D.J. performed mRNA expression analyses.

N.Kishimoto, D.W.S., and J.W. performed immunofluorescence studies.

S.B.S., F.C.L. and R.S. performed *Rfx6* gene targeting studies.

S.B.S. performed DNA binding and transcription studies.

H.Q.Q. performed homozygosity mapping.

N.T., R.M.G., K.D. and J.W. performed Nimblegen array and sequencing studies.

A.M.P., J.M, J.D, S.V.E., M.A., N. Kacet, J.W., M.E.R., M.G., I.H., and A. H. recruited the human subjects and provided phenotypic information.

Competing interests M.S.G. is an inventor on patents held by the University of California covering Neurogenin3 and its use.

¹²Department of Medicine, University of California San Francisco, San Francisco, CA 94143, U.S.A.

Abstract

Insulin from the β -cells of the pancreatic islets of Langerhans controls energy homeostasis in vertebrates, and its deficiency causes diabetes mellitus. During embryonic development, the transcription factor Neurogenin3 initiates the differentiation of the β -cells and other islet cell types from pancreatic endoderm, but the genetic program that subsequently completes this differentiation remains incompletely understood. Here we show that the transcription factor Rfx6 directs islet cell differentiation downstream of Neurogenin3. Mice lacking Rfx6 failed to generate any of the normal islet cell types except for pancreatic-polypeptide-producing cells. In human infants with a similar autosomal recessive syndrome of neonatal diabetes, genetic mapping and subsequent sequencing identified mutations in the human *RFX6* gene. These studies demonstrate a unique position for Rfx6 in the hierarchy of factors that coordinate pancreatic islet development in both mice and humans. Rfx6 could prove useful in efforts to generate β -cells for patients with diabetes.

During embryonic development, the pancreas first appears as clusters of cells on the dorsal and ventral aspects of the gut endoderm. The exocrine and endocrine cells that form the adult pancreas differentiate from this pool of pancreatic progenitors ¹. A single transcription factor, the pro-endocrine bHLH factor Neurogenin3, is both necessary and sufficient to drive these progenitor cells to differentiate into the endocrine cells that form the islets of Langerhans ^{2,3,4}. Transient activation of Neurogenin3 expression in scattered progenitor cells initiates expression of additional transcription factors, including NeuroD1, Pax4, Nkx2.2, Nkx6.1, Arx, and others, which then direct the differentiation of those cells into the distinct islet cell subtypes and the activation of the mature islet transcription factors such as MafA, Pax6 and Isl1 ¹. Mutations in many of these genes can cause diabetes, highlighting the pathway's importance in human beta-cell formation and insulin production⁵. Understanding and controlling this process of differentiation may ultimately provide us with the cells needed to treat diabetes mellitus.

Expression of Rfx6

In independent screens for genes co-expressed with Neurogenin3 in islet progenitor cells ⁶, activated by Neurogenin3 ⁷, and uniquely expressed in islets (M.E.W. and J.D.J., unpublished data), we identified Rfx6, a member of the RFX (Regulatory Factor X-box binding) family of winged-helix transcription factors ^{8,9}. *Rfx6* transcripts could be detected in mouse and human embryonic pancreas by RT-PCR (Fig. 1a,b), but, unlike all other known islet transcription factors, not in brain (Fig. 1a, c), and not in mouse embryonic pancreas lacking Neurogenin3 (Fig. 1d). In contrast, mouse *Rfx4*, the mammalian RFX gene with the highest homology to *Rfx6*, was amplified from brain and not from pancreas, and the other RFX genes were more widely expressed (Fig.1a).

To explore the pattern of Rfx6 protein expression, we used antiserum generated against recombinant Rfx6 protein for immunofluorescence studies. In mice, Rfx6 was detected as

early as embryonic day 7.5 (e7.5) throughout the definitive, but not extraembryonic, endoderm and persisted broadly in gut endoderm at e9.0, after which it becomes progressively restricted to the pancreas and scattered cells in the gut (Fig. 2a-c, Supplemental Fig. S1 and data not shown). At e10.0, immunofluorescence staining detected Rfx6 in foregut/midgut epithelium and in scattered cells in the nascent pancreatic buds, as indicated by staining for pancreatic transcription factor Pdx1 (Fig. 2d-f). Most of these scattered Rfx6-expressing cells did not co-express Pdx1, but many co-expressed Nkx2.2 and Neurogenin3 (Supplemental Figs. S1 and S2). By e12.5, the Rfx6-expressing cells were generally distinct from the Pdx1-expressing progenitor cells, but most co-expressed glucagon, demonstrating restricted expression of Rfx6 in the endocrine lineage even at this early stage (Supplemental Fig. S3). In pancreata from Neurog3^{-/-} embryos¹⁰, there were no Rfx6-expressing cells (Supplemental Fig. S4).

During the peak of endocrine cell differentiation at e15.5, Rfx6 co-localized with Neurogenin3 in the nuclei of a subset of the endocrine progenitor cells (Fig 2g), and overlapped with the islet transcription factors Nkx2.2, Nkx6.1, and Pdx1 (Supplemental Fig. S5). At e18.5, Rfx6 could be found in the nuclei of cells expressing each of the major pancreatic endocrine hormones (Fig. 2h and Supplemental Fig. S6). In the adult pancreas, Rfx6 expression was restricted to the islets where it could be detected in all endocrine lineages (Fig.2i and Supplemental Fig. S7).

To generate Rfx6 null mice, we used homologous recombination to replace the first five exons of the Rfx6 gene, including the sequences encoding the DNA-binding domain, with a cassette encoding an eGFP-cre fusion protein (Supplementary Fig. S8). By crossing mice heterozygous for the mutant allele with mice carrying the marker gene *ROSA26 loxP-stop-loxP lacZ (R26R)*¹¹, we generated *Rfx6^{+eGFPcre}/R26R* double heterozygous mice in which Rfx6-expressing cells and their descendants are marked by the expression of β -galactosidase and can be visualized with the X-gal substrate (Fig. 3a-d and Supplemental Fig. S9). β -galactosidase expression was detected in all embryonic tissue derived from the endoderm germ layer, but not in other embryonic or in extraembryonic tissues, demonstrating that Rfx6 is broadly expressed in and restricted to the definitive endoderm prior to the formation of the endoderm-derived organs. Taken together, the immunohistochemistry data and lineage tracing demonstrate that Rfx6 is expressed initially broadly in the definitive endoderm after gastrulation, becomes restricted to the gut and pancreatic bud at mid gestation, is reactivated by Neurogenin3 in islet progenitor cells and is ultimately restricted to pancreatic islets in the mature pancreas.

***Rfx6^{eGFPcre/eGFPcre}* mice**

From heterozygous crosses, homozygous *Rfx6^{eGFPcre/eGFPcre}* mice were born at the expected Mendelian ratio, but failed to feed normally, exhibited gross bowel distension due to small bowel obstruction (Fig. 3e-f) and died within 2 days post partum. Some, but not all, of the Rfx6 null animals also had reduced pancreas size (data not shown).

To test for effects on gene expression prior to birth, we harvested RNA from e17.5 pancreata, and used low density TaqMan arrays⁶ to measure the levels of a set of pancreatic

genes (Supplemental Table S1). *Rfx6*^{eGFPcre/GFPcre} pancreata had almost no expression of the islet hormones genes, except for pancreatic polypeptide (*Ppy*). Several other islet/β-cell genes, such as the zinc transporter *Slc30a8* and G-protein coupled receptor *GPR40/Ffar* genes, were similarly reduced; but other β-cell genes were more modestly reduced, including the glucose sensing genes *Gck*, *Slc2a2*, and *Kcnj11*. Immunofluorescence staining with the endocrine markers Chromogranin A or Synaptophysin at e17.5 demonstrated that the *Rfx6*^{eGFPcre/eGFPcre} pancreata still contained a large number of endocrine cells, but confirmed that none of these cells expressed insulin, glucagon, somatostatin or ghrelin (Fig. 4). Although the number of *Ppy*-expressing cells was increased in the *Rfx6*^{eGFPcre/eGFPcre} pancreata, they only accounted for a subset of the endocrine cells (Fig. 4i-l), leaving the identity of the remaining endocrine cells unknown.

We also tested whether *Rfx6* regulates other transcription factor genes (Supplemental Table S2). The absence of *Rfx6* did not affect *Neurogenin3* expression, and this was confirmed at the protein level (data not shown). In sharp contrast, expression of genes downstream of *Neurogenin3* encoding factors involved in alpha-cell development, including *Irx2* and *Arx*, was markedly reduced in *Rfx6*^{eGFPcre/eGFPcre} pancreata.

Interestingly, genes encoding several factors involved in insulin gene transcription (*Pax6*, *MafA*, *NeuroD1* and *Pdx1*) also had reduced expression, but some key genes involved in β-cell specification either did not significantly change (*Nkx2.2* and *Nkx6.1*), or increased (*Pax4*). Immunofluorescence staining at e17.5 revealed that the field of *Nkx6.1* expression expanded from β-cells alone in wildtype pancreata to include all of the Chromogranin A + endocrine cells, including the PP cells in *Rfx6*^{eGFPcre/eGFPcre} pancreata (Fig. 4i-l and Supplementary Table S3). These studies suggest that while *Rfx6* regulates the transcription factors involved in β-cell maturation and function, it restricts the expression of the β-cell differentiation and specification genes, and thus the β-cell fate choice.

Mice with a targeted disruption of the *Rfx3* gene have an islet phenotype that is similar to, but less extreme than, the *Rfx6*^{eGFPcre/eGFPcre} mice, with reductions in the numbers, but not complete loss, of insulin- and glucagon-expressing cells and an increase in pancreatic polypeptide-expressing cells¹². In a proteome-wide screen of protein-protein interactions, *Rfx6* was found to interact with *Rfx2* and *3*¹³. Since the RFX transcription factors generally bind to their target DNA sites (the “X box”) as dimers¹⁴, we tested whether *Rfx6* and *Rfx3* form a heterodimeric DNA binding complex in an electromobility shift assay (EMSA). We found that both full length *Rfx3*, and truncations that retain the DNA-binding and dimerization domains, bound to an X box site together with *Rfx6* (Fig. 5a and Supplementary Fig. S10), and that the two factors cooperated in activating a promoter containing multimers of this X box site (Fig 5b).

It has been proposed that the islet phenotype of the *Rfx3*^{-/-} mice results from defects in primary cilia formation on islet cells¹², although islets lacking any primary cilia develop fairly normally^{15,16}. Unlike in the *Rfx3*^{-/-} mice, we found that primary cilia formation was unaffected in the *Rfx6*^{eGFPcre/eGFPcre} islets (Supplementary Fig. 11a-d). In addition, expression of the cilia genes *Ift88* and *Dync2li1*, which are reduced in the pancreas of *Rfx3*^{-/-} mice¹², was not reduced in the pancreas of *Rfx6*^{eGFPcre/eGFPcre} mice (Supplementary Fig.

11e). We conclude that Rfx3 and Rfx6 cooperate in regulating a set of genes involved in islet development but not in cilia formation. The more modest islet phenotype in the *Rfx3*^{-/-} mice may be due to the ability of Rfx2 to compensate partially for the loss of Rfx3 (Fig. 1a), or the ability of Rfx6 to direct gene expression as a homodimer (Fig. 5a, b).

Human mutations in *RFX6*

The phenotype of the *Rfx6*^{eGFPcre/eGFPcre} mice is remarkably similar to human patients born with neonatal diabetes and small bowel obstruction due to bowel atresia^{17, 18}. Despite some reduction in pancreatic size, these cases were not deficient in enzymes of the exocrine pancreas, and autopsies of two cases (proband #1 and case 3 in Ref¹⁷) revealed normal-appearing exocrine pancreata with clusters of ChromograninA-positive cells but total absence of cells staining for insulin, glucagon, or somatostatin¹⁷. In addition, the syndrome involves hypoplastic gall bladder, and intractable diarrhea unresponsive to pancreatic enzyme replacement.

The disease locus was mapped using overlapping homozygosity in probands #1 and #2 (see Supplementary material for pedigree information and references to previous clinical case reports) respectively the offspring of first and second cousins. High-resolution homozygosity mapping identified 10 homozygosity-by-descent (HBD) segments >500 kb in proband #1 (after excluding those that overlapped with her unaffected sibling, Supplementary Table S4), and 25 HBD segments >500kb in proband #2 (Supplementary Table S5). Only three HBD regions were common in the two probands, totaling 24 Mb (Table 1). Altogether, 194 RefSeq genes map to these regions. Of these genes, only *RFX6*, which falls in the largest segment at 6q21-22, had pancreas-enriched expression in the TiGER database¹⁹ (Supplementary Table 6), and also increased in expression in human pancreas between foetal ages 10 and 20 weeks (Fig. 1b and Supplementary Figs. S13 and S14), concordant with the appearance of endocrine cells^{20,21}.

Two parallel, independent approaches unequivocally identified mutations in the *RFX6* gene in this human syndrome: direct sequencing of the *RFX6* gene and unbiased deep sequencing of all exons within the three overlapping HBD regions.

For deep sequencing, exons were captured from DNA obtained from Proband #2 using a tiled oligonucleotide array²² covering 1,309 of 1,322 exons mapping within the HBD regions²³. Amplification and sequencing²⁴ of the captured fragments generated 40,379 sequences of at least 100 bp that aligned within the target regions. Median target coverage depth was 9.2, with 80% of targets having a depth of at least 4. Given that we were searching for a homozygous mutation, this was sufficient for unequivocal detection of exonic variants. Altogether, 30 novel sequence variants were detected (Supplementary Table S7): 15 in introns, 3 in both introns and untranslated regions (UTRs), 9 in UTRs, and only three in coding sequences, two synonymous. The only non-synonymous variant was 217 Ser>Pro in *RFX6*, identifying this gene as the most likely candidate.

In parallel, direct sequencing was performed on the 19 exons and the splicing junctions of *RFX6* in all probands. Missense, splicing or frameshift mutations in *RFX6* were found in five of the six available probands (Fig. 5e) with an interesting genotype-phenotype

correlation. Proband #1, 4 and 5 all died in the first few months of life and were homozygous for, respectively, a loss of the donor splicing site in intron 2 (IVS2+2 t>c), an out-of-frame deletion in exon 7, and the missense mutation 181 R>Q involving a highly conserved arginine in the DNA-binding domain^{8,25}(Supplementary Fig. S15). Proband #3, still alive at the age of 9 and intermittently off insulin, was a compound heterozygote for donor-site loss in intron 6 (IVS6+2 t>g) and disruption of the acceptor site in intron 1 (IVS1-12 a>g). Proband #2, still alive at age 4.5 years¹⁸, had the homozygous missense mutation 217 Ser>Pro, confirming the unbiased exon sequencing described above. All mutations were inherited from carrier parents.

To determine the significance of the homozygous intron 2 splice donor splicing site mutation in proband #1, we amplified *RFX6* mRNA by RT-PCR of high-quality RNA from autopsy pancreas and failed to detect the properly spliced transcript, which was easily amplified from normal foetal pancreas as was the reference gene cyclophilin in the proband's RNA. We also failed to detect any RNA from exons 1+2, upstream of the splicing mutation, probably due to nonsense-mediated decay²⁶(Supplementary Fig. S16).

We also tested the two missense mutations for their effect on DNA binding by Rfx6. We found that 181R>Q (proband #5), which alters a conserved amino acid in the DNA binding domain, completely abrogated DNA binding, while 217S>P (proband #2), which lies between the DNA-binding domain and dimerization domain of Rfx6, only modestly reduced DNA binding (Fig. 5d) and did not affect dimer formation (data not shown).

Finally, we failed to identify any mutation in *RFX6* in proband #6. In the absence of DNA from the proband, we sequenced both parents and found no point mutation of *RFX6* or *NEUROG3*; and long-range PCR did not reveal any deletions of *RFX6* (Supplementary Fig. S17). In the absence of proband DNA we cannot rule out a *de novo* mutation, but this case is most likely a phenocopy. We also failed to find *RFX6* mutations in a case of the Martinez-Frias syndrome²⁷. Finally, a search of the *RFX6* linkage disequilibrium block in our genome-wide association data^{28,29}, combined with those of the WTCC³⁰, did not reveal any common variants associated with type 1 or type 2 diabetes (data not shown).

Discussion

In the pancreas, Rfx6 acts downstream of the pro-endocrine factor Neurogenin3 (Fig. 5c), and mutation of the two genes give similar but distinct phenotypes. Like *RFX6* mutations, mutation of *NEUROG3* in humans also causes intractable diarrhoea and diabetes³¹, but *NEUROG3* mutation does not cause the small bowel atresia or biliary abnormalities seen with *RFX6* mutation, which is not surprising since Neurogenin3 is not expressed in the early gut endoderm as is Rfx6^{4,32,33}. Despite severe intestinal malabsorption, pancreatic exocrine function is intact in both syndromes, and the only histological abnormality in the gut in the mutant *NEUROG3* syndrome is loss of the intestinal endocrine cells³⁴. Comparison of the gut endocrine cells affected by these two related syndromes may provide new insight into mechanisms that regulate nutrient absorption in the small bowel.

In addition, *RFX6* mutations cause diabetes at birth, while the reported patients with homozygous mutations in Neurogenin3 did not develop diabetes until several years later³¹, despite evidence that Neurogenin3 is absolutely required for the generation of islet cells and production of insulin in mice². Incomplete loss of function in the reported human *NEUROG3* mutations could explain the continued insulin production in these patients³⁵. Alternatively, recent evidence that *Neurog3*^{-/-} mice still generate a small number of islet cells³⁶ suggests some redundancy of Neurogenin3's pro-endocrine function, possibly due to the presence of related bHLH proteins in the pancreas^{4,7}. In contrast, our data do not indicate any redundancy of Rfx6 function in endocrine differentiation and demonstrate remarkable conservation of the genetic control of islet development, despite some discrepancy between mouse and human *NEUROG3* mutants.

It should be noted that our patients with *RFX6* mutations have some similarities with other reported cases, especially those with the Martinez-Frias syndrome (MFS)²⁷, under which OMIM currently lists our cases. However, since the original MFS patients also had oesophageal atresia and hypospadias, and did not have diabetes, and we did not find any *RFX6* mutation in the parents of one case of MFS, our cases are distinct from MFS. We propose to name their condition, now of defined molecular aetiology, the *Mitchell-Riley* syndrome after the two clinicians who first described it¹⁷.

In summary, we have identified a novel factor in endoderm and islet development, Rfx6, that is required for the differentiation of 4 of the 5 islet cell types and for the production of insulin in both humans and mice. In the hierarchy of islet developmental factors, it lies downstream of Neurogenin3 and upstream of many of the other islet transcription factors (Fig. 4d). A full understanding of the role of Rfx6 will help to clarify how islets and β -cells are generated, what goes wrong in this process in diabetes, and how to generate new β -cells for patients with diabetes.

Methods summary

All studies involving mice were approved by the UCSF Institutional Animal Care and Use Committee. Timed matings were carried out with embryonic day 0.5 being set as midday of the day of discovery of a vaginal plug. The Rfx6 targeting allele (Supplementary Fig. S8) was generated by recombineering in a modified bacterial artificial chromosome followed by recombination into plasmid DNA by gap-repair³⁸. This construct was used by the UCSF DERC Transgenic Core Laboratory to target the *Rfx6* allele in 129 (E14) mouse embryonic stem cells, which were injected into mouse blastocysts to generate chimeric *Rfx6*^{+/*eGFPcre*} mice. Chimeras and subsequent generations were crossed to C57BL/6 mice. Mouse tissue processing, β -galactosidase detection, immunofluorescence staining³⁹, automated cell counting⁴⁰, transfections of mPAC cells, EMSA⁴¹ and mRNA quantification with low density TaqMan arrays⁶ were performed as previously described. All antisera used for immunofluorescence studies are listed in Supplementary Table S8. Sequences of oligonucleotides used for RT-PCR, ESC colony screening, mouse genotyping and EMSA are available on request.

The human subjects protocol was approved by the IRB of the Montreal Children's Hospital and written informed consent was obtained from all participating families. Clinical findings and case-report references are summarized in the web supplement. For homozygosity mapping, results from the *Illumina* Hap 550 (proband #1, call rate 0.99) or 1M (proband #2, call rate 0.978) microarrays³⁷, were used to scan autosomes in 300-kb windows and HBD was defined as absence of any heterozygous SNP in the proband and presence of at least one in either parent or the unaffected sibling. Long-oligo Nimblegen capture arrays²² included around 100 bp extension of intronic sequence coverage from the boundary of the exons. The eluted enriched regions from proband #1 were run on the Roche 454 FLX Genome Sequencer²⁴. The 19 exons of *RFX6* were PCR-amplified manually for Sanger sequencing in the remaining probands. For the long range PCR, we used the Kit # K0182 from *Fermentas* for fragments ranging from 6 to 17 Kb (Supplementary Fig S17).

Supplementary Material

Refer to Web version on PubMed Central for supplementary material.

Acknowledgements

We thank all the patients and their families for the participation in this study and Dr. Patricia Riley for allowing us access to her clinical data. We thank G. Grodsky, G. Bell, W. Rutter, R. Gasa and members of the German laboratory for helpful discussions, F. Schauffle and the DERC Microscopy Core Laboratory, C. Mrejen and the UCSF DERC Genomics Core, N. Killeen and the UCSF DERC Transgenic Core Laboratory for help with the generation of the *Rfx6*-targeted mice, Regina Koshy for technical assistance, Y. Zhang and S. Zhao for assistance with mouse husbandry and genotyping, the Massively Parallel Sequencing team at the McGill University and Genome Quebec Innovation Center for DNA sequencing and Jessica Wasserscheid for bioinformatics analyses. This work was supported by grants from the Larry L. Hillblom Foundation (S.B.S. and M.S.G.), the Juvenile Diabetes Research Foundation (S.B.S., F.C.L., T.M., C.P., and M.S.G.), the American Diabetes Association (M.S.G.), the Nora Eccles Treadwell Foundation (M.S.G.), the Canadian Institutes of Health Research (H.Q.Q.), and the National Institutes of Health/National Institute of Diabetes and Digestive and Kidney Diseases (M.S.G.).

References

1. Murtaugh LC. Pancreas and beta-cell development: from the actual to the possible. *Development*. 2007; 134:427–438. [PubMed: 17185316]
2. Gradwohl G, Dierich A, LeMeur M, Guillemot F. neurogenin3 is required for the development of the four endocrine cell lineages of the pancreas. *Proc Natl Acad Sci U S A*. 2000; 97:1607–1611. [PubMed: 10677506]
3. Apelqvist A, et al. Notch signaling controls pancreatic cell differentiation. *Nature*. 1999; 400:877–881. [PubMed: 10476967]
4. Schwitzgebel VM, et al. Expression of neurogenin3 reveals an islet cell precursor population in the pancreas. *Development*. 2000; 127:3533–3542. [PubMed: 10903178]
5. McCarthy MI, Hattersley AT. Learning from molecular genetics: novel insights arising from the definition of genes for monogenic and type 2 diabetes. *Diabetes*. 2008; 57:2889–2898. [PubMed: 18971436]
6. Miyatsuka T, Li Z, German MS. Chronology of islet differentiation revealed by temporal cell labeling. *Diabetes*. 2009; 58:1863–1868. [PubMed: 19478145]
7. Gasa R, et al. Induction of pancreatic islet cell differentiation by the neurogenin-neuroD cascade. *Differentiation; research in biological diversity*. 2008; 76:381–391.
8. Aftab S, Semene L, Chu JS, Chen N. Identification and characterization of novel human tissue-specific RFX transcription factors. *BMC Evol Biol*. 2008; 8:226. [PubMed: 18673564]

9. Emery P, Durand B, Mach B, Reith W. RFX proteins, a novel family of DNA binding proteins conserved in the eukaryotic kingdom. *Nucleic acids research*. 1996; 24:803–807. [PubMed: 8600444]
10. Lee CS, Perreault N, Brestelli JE, Kaestner KH. Neurogenin 3 is essential for the proper specification of gastric enteroendocrine cells and the maintenance of gastric epithelial cell identity. *Genes & development*. 2002; 16:1488–1497. [PubMed: 12080087]
11. Soriano P. Generalized lacZ expression with the ROSA26 Cre reporter strain. *Nature genetics*. 1999; 21:70–71. [PubMed: 9916792]
12. Ait-Lounis A, et al. Novel function of the ciliogenic transcription factor RFX3 in development of the endocrine pancreas. *Diabetes*. 2007; 56:950–959. [PubMed: 17229940]
13. Rual JF, et al. Towards a proteome-scale map of the human protein-protein interaction network. *Nature*. 2005; 437:1173–1178. [PubMed: 16189514]
14. Emery P, et al. A consensus motif in the RFX DNA binding domain and binding domain mutants with altered specificity. *Molecular and cellular biology*. 1996; 16:4486–4494. [PubMed: 8754849]
15. Cano DA, Sekine S, Hebrok M. Primary cilia deletion in pancreatic epithelial cells results in cyst formation and pancreatitis. *Gastroenterology*. 2006; 131:1856–1869. [PubMed: 17123526]
16. Cano DA, Murcia NS, Pazour GJ, Hebrok M. Orpk mouse model of polycystic kidney disease reveals essential role of primary cilia in pancreatic tissue organization. *Development*. 2004; 131:3457–3467. [PubMed: 15226261]
17. Mitchell J, et al. Neonatal diabetes, with hypoplastic pancreas, intestinal atresia and gall bladder hypoplasia: search for the aetiology of a new autosomal recessive syndrome. *Diabetologia*. 2004; 47:2160–2167. [PubMed: 15592663]
18. Chappell L, et al. A further example of a distinctive autosomal recessive syndrome comprising neonatal diabetes mellitus, intestinal atresias and gall bladder agenesis. *Am J Med Genet A*. 2008; 146A:1713–1717. [PubMed: 18512226]
19. Liu X, Yu X, Zack DJ, Zhu H, Qian J. TiGER: a database for tissue-specific gene expression and regulation. *BMC Bioinformatics*. 2008; 9:271. [PubMed: 18541026]
20. Stefan Y, Grasso S, Perrelet A, Orci L. A quantitative immunofluorescent study of the endocrine cell populations in the developing human pancreas. *Diabetes*. 1983; 32:293–301. [PubMed: 6131849]
21. Lyttle BM, et al. Transcription factor expression in the developing human fetal endocrine pancreas. *Diabetologia*. 2008; 51:1169–1180. [PubMed: 18491072]
22. Hodges E, et al. Genome-wide in situ exon capture for selective resequencing. *Nat Genet*. 2007; 39:1522–1527. [PubMed: 17982454]
23. Karolchik D, et al. The UCSC Genome Browser Database: 2008 update. *Nucleic Acids Res*. 2008; 36:D773–779. [PubMed: 18086701]
24. Albert TJ, et al. Direct selection of human genomic loci by microarray hybridization. *Nat Methods*. 2007; 4
25. Gajiwala KS, et al. Structure of the winged-helix protein hRFX1 reveals a new mode of DNA binding. *Nature*. 2000; 403:916–921. [PubMed: 10706293]
26. Chang YF, Imam JS, Wilkinson MF. The nonsense-mediated decay RNA surveillance pathway. *Annu Rev Biochem*. 2007; 76:51–74. [PubMed: 17352659]
27. Gentile M, Fiorente P. Esophageal, duodenal, rectoanal and biliary atresia, intestinal malrotation, malformed/hypoplastic pancreas, and hypospadias: further evidence of a new distinct syndrome. *Am J Med Genet*. 1999; 87:82–83. [PubMed: 10528254]
28. Hakonarson H, et al. A novel susceptibility locus for type 1 diabetes on Chr12q13 identified by a genome-wide association study. *Diabetes*. 2008; 57:1143–1146. [PubMed: 18198356]
29. Sladek R, et al. A genome-wide association study identifies novel risk loci for type 2 diabetes. *Nature*. 2007; 445:881–885. [PubMed: 17293876]
30. Genome-wide association study of 14,000 cases of seven common diseases and 3,000 shared controls. *Nature*. 2007; 447:661–678. [PubMed: 17554300]
31. Wang J, et al. Mutant neurogenin-3 in congenital malabsorptive diarrhea. *The New England journal of medicine*. 2006; 355:270–280. [PubMed: 16855267]

32. Jensen J, et al. Independent development of pancreatic alpha- and beta-cells from neurogenin3-expressing precursors: a role for the notch pathway in repression of premature differentiation. *Diabetes*. 2000; 49:163–176. [PubMed: 10868931]
33. Gu G, Dubauskaite J, Melton DA. Direct evidence for the pancreatic lineage: NGN3+ cells are islet progenitors and are distinct from duct progenitors. *Development*. 2002; 129:2447–2457. [PubMed: 11973276]
34. Cortina G, et al. Enteroendocrine cell dysgenesis and malabsorption, a histopathologic and immunohistochemical characterization. *Hum Pathol*. 2007; 38:570–580. [PubMed: 17258790]
35. Jensen JN, Rosenberg LC, Hecksher-Sorensen J, Serup P. Mutant neurogenin-3 in congenital malabsorptive diarrhea. *The New England journal of medicine*. 2007; 356:1781–1782. author reply 1782. [PubMed: 17460236]
36. Wang S, et al. Myt1 and Ngn3 form a feed-forward expression loop to promote endocrine islet cell differentiation. *Dev Biol*. 2008; 317:531–540. [PubMed: 18394599]
37. Steemers FJ, Gunderson KL. Whole genome genotyping technologies on the BeadArray platform. *Biotechnol J*. 2007; 2:41–49. [PubMed: 17225249]
38. Copeland NG, Jenkins NA, Court DL. Recombineering: a powerful new tool for mouse functional genomics. *Nat Rev Genet*. 2001; 2:769–779. [PubMed: 11584293]
39. Nekrep N, Wang J, Miyatsuka T, German MS. Signals from the neural crest regulate beta-cell mass in the pancreas. *Development*. 2008; 135:2151–2160. [PubMed: 18506029]
40. Lynn FC, et al. MicroRNA expression is required for pancreatic islet cell genesis in the mouse. *Diabetes*. 2007; 56:2938–2945. [PubMed: 17804764]
41. Lynn FC, et al. Sox9 coordinates a transcriptional network in pancreatic progenitor cells. *Proc Natl Acad Sci U S A*. 2007; 104:10500–10505. [PubMed: 17563382]
42. David E, Garcia AD, Hearing P. Interaction of EF-C/RFX-1 with the inverted repeat of viral enhancer regions is required for transactivation. *J Biol Chem*. 1995; 270:8353–8360. [PubMed: 7713944]

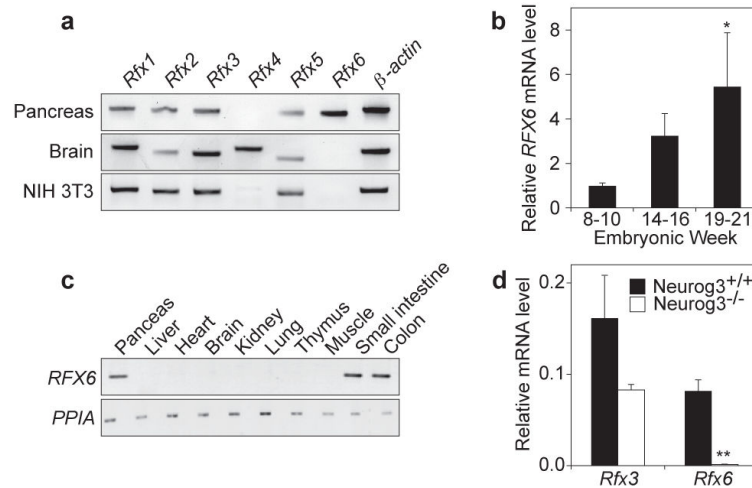


Figure 1. Expression of *Rfx6* in mice and human tissues

In a, the mRNA for *Rfx* genes 1-6 were amplified by RT-PCR from RNA isolated from the pancreas and brain of mouse embryos at e17.5 and from NIH3T3 fibroblasts. In b, levels of *RFX6* mRNA were determined by real-time PCR of RNA from whole pancreas of human foetuses at the ages shown. n= 5 samples per foetal age group. *p= 0.017, weeks 8-10 vs. 19-21, by two-tailed Student's t test. In c, mRNA for *RFX6* and control gene *Cyclophilin A* (*PPIA*) genes were amplified by RT-PCR from RNA isolated from the human adult tissues shown. In d, levels of *Rfx3* and *Rfx6* mRNA were determined by real-time RT-PCR (TaqMan) of RNA isolated from the pancreata of wildtype and *Neurog3*^{-/-} mouse embryos at e17.5 values and expressed relative to the level of *Gusb*. n= 3 samples per group. **p = 0.0025, wildtype vs. mutant, by two-tailed Student's t test.

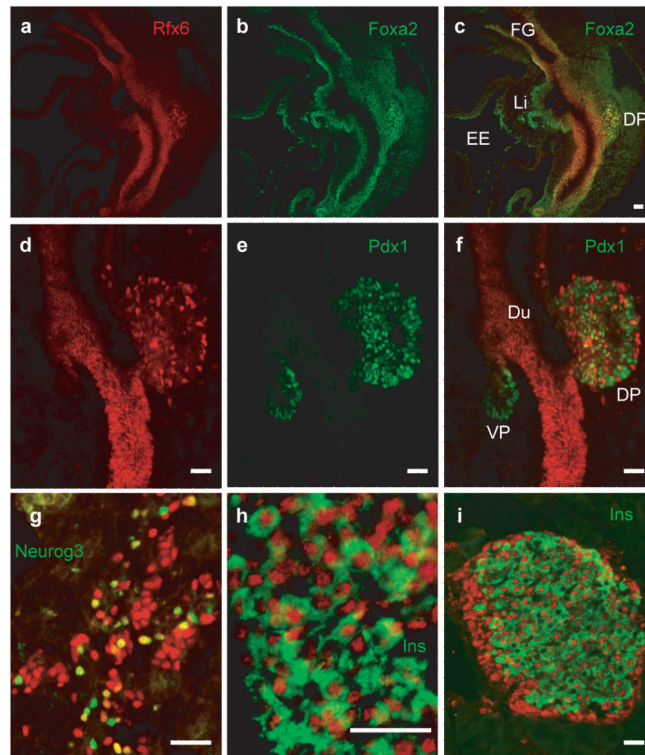


Figure 2. Expression of Rfx6 in mice

Immunofluorescence staining was performed for Rfx6 (red) in mouse embryos. In a - c, at e9, Rfx6 staining overlaps with Foxa2 in the gut epithelium (including foregut, FG) and nascent dorsal pancreatic bud (DP), but Foxa2 is expressed alone in the liver bud (Li) and extraembryonic endoderm (EE). Separate colour channels are shown for red (a and d) and green (b and e). In d - f, costaining was performed with Pdx1 (green) in gut (duodenum, Du), dorsal pancreas (DP) and ventral pancreas (VP) at e10. In g, e15.5 pancreas was costained for Neurogenin3 (green). Costaining nuclei appear yellow. In h, e18.5 pancreas was costained for insulin (green). In i, adult pancreas was costained for insulin (green). Higher resolution photomicrographs from additional dates with additional markers can be found in Supplementary Figs. 1-7. Scale bars, 25 μ m.

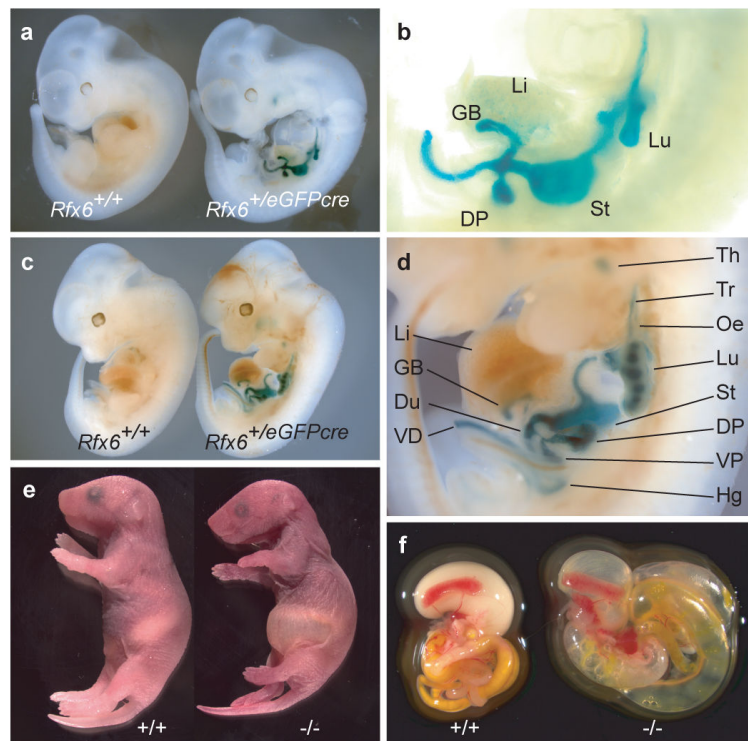


Figure 3. Targeting of the *Rfx6* gene in mice

In panel a-d, lineage tracing was performed on *Rfx6*^{+/+}/*R26R* (left in a and c) or *Rfx6*^{+/*eGFPcre*}/*R26R* (b and d, and right in a and c) mice at e10.5 (a, b) and e12.5 (c, d) by staining for β -galactosidase activity with Xgal (blue). Panel b shows a close-up view of the animal on the right in panel a, and panel d shows a close-up view of the animal on the right in panel c. In panel e, an *Rfx6*^{*eGFPcre/eGFPcre*} pup at p2 is shown on the right, with a wildtype litter mate on the left. In panel f, the dissected abdominal viscera are shown for wildtype (left) and *Rfx6*^{*eGFPcre/eGFPcre*} (right) pups at p0.5. Additional photographs of the lineage tracing and mutant animals can be found in Supplementary Fig. 10. Li, liver; Du, duodenum; GB, gall bladder; VD, vitelline duct; Th, thymus; Tr, trachea; Oe, oesophagus; Lu, lung; St, stomach; DP, dorsal pancreas; VP, ventral pancreas; Hg, hindgut.

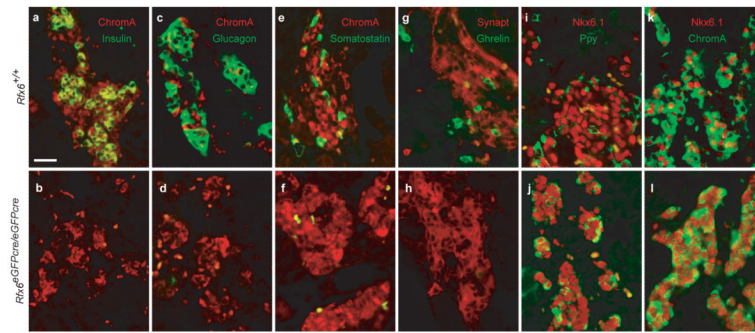


Figure 4. Expression patterns of islet markers in wildtype and *Rfx6^{eGFPcre/eGFPcre}* mice at e17.5 On pancreas sections from e17.5 embryos with the genotypes shown at the left, immunofluorescence costaining was performed for ChromograninA (ChromA, red, a - f, green k, l), Synaptophysin (Syn, red, g, h), insulin (green, a, b), glucagon (green, c, d), somatostatin (Sst, green, e, f), ghrelin (green g, h), Nkx6.1 (red in i - l), and pancreatic polypeptide (Ppy, green, k, l). Quantification of cells expressing Ppy and Nkx6.1 is shown in Supplementary Table S3. Scale bars, 25 μ m.

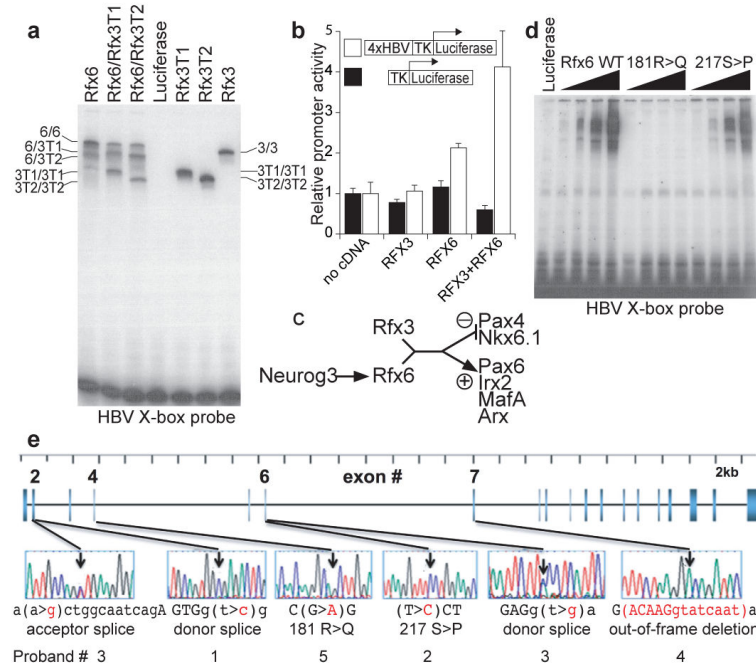


Figure 5. Function of the human Rfx6 protein

In a and c, DNA binding of the human *in vitro*-translated proteins shown above each lane to the double-stranded, radiolabeled oligonucleotide HBV X-box probe⁴² was tested by electromobility shift assay (EMSA). In a, combined proteins were co-translated, and probe bound by the heterodimer partners has a mobility between that of the two homodimers. Truncated proteins Rfx3T1 and Rfx3T2 have the first 119 and 160 amino-terminal amino acids removed respectively, but retain the DNA-binding and dimerization domains. *In vitro*-translated luciferase is included as a negative control. A close-up view of a longer gel is shown in Supplementary Fig. S10a. In b, mouse pancreatic ductal mPac L20 cells were co-transfected with a DNA plasmid containing the reporter constructs shown and another expressing the RFX cDNAs shown, luciferase reporter expression was assayed for each combination. *p = 0.0026 vs. “no cDNA”, 0.0024 vs. Rfx3 alone, and 0.011 vs. Rfx6 alone by two-tailed Student’s t test. In c, a schematic shows the proposed interactions, either direct or indirect, of several transcription factors during pancreas development. In d, increasing amounts of the *in vitro*-translated human Rfx6 wild type and R181Q and S217P mutant proteins were assayed for binding to the X-box DNA probe. Efficiency of mutant protein production is demonstrated in Supplementary Fig. S10b. In e, mutations found in patients are indicated on a map of the RFX6 gene. All mutations were homozygous except for proband 3.

Table 1

Regions of homozygosity-by-descent common to probands #1 and #2

Chromosome	start SNP	start position	end SNP	end position	Size
2p15-16	rs6754038	57,761,104	rs1426699	64,418,856	6,657,752
6q21-22	rs6913656	112,589,928	rs10499129	124,975,906	12,385,978
6q23	rs7744295	131,173,627	rs17065195	136,360,914	5,187,287